Confined states in multiple quantum well structures of Si_nGe_n nanowire superlattices

N. Akman,[1] E. Durgun,[2,3] S. Cahangirov,[3] and S. Ciraci[2,3,*]
[1]*Department of Physics, Mersin University, Mersin 33343, Turkey*
[2]*Department of Physics, Bilkent University, Ankara 06800, Turkey*
[3]*UNAM-Institute for Materials Science and Nanotechnology, Bilkent University, Ankara 06800, Turkey*
(Received 7 September 2007; published 21 December 2007)

Mechanical properties, atomic and energy band structures of bare and hydrogen-passivated Si_nGe_n nanowire superlattices have been investigated by using first-principles pseudopotential plane-wave method. Undoped, tetrahedral Si and Ge nanowire segments join pseudomorphically and can form superlattice with atomically sharp interface. We found that Si_n nanowires are stiffer than Ge_n nanowires. Hydrogen passivation makes these nanowires and Si_nGe_n nanowire superlattice even more stiff. Upon heterostructure formation, superlattice electronic states form subbands in momentum space. Band lineups of Si and Ge zones result in multiple quantum wells, where specific states at the band edges and in band continua are confined. The electronic structure of the nanowire superlattice depends on the length and cross section geometry of constituent Si and Ge segments. Since bare Si and Ge nanowires are metallic and the band gaps of hydrogenated ones vary with the diameter, Si_nGe_n superlattices offer numerous alternatives for multiple quantum well devices with their leads made from the constituent metallic nanowires.

DOI: 10.1103/PhysRevB.76.245427 PACS number(s): 61.46.−w, 68.65.Cd, 73.20.At, 73.21.Fg

I. INTRODUCTION

Planar superlattices have been fabricated either through periodic junction of alternating semiconductor layers with different band gaps or through repeating compositional modulation. Electrons in parallel layers show two-dimensional (2D) free electronlike behavior and have quantization different from those three-dimensional bulk semiconductors. Minibands in the momentum space in the direction perpendicular to the layers and periodically varying band gap in the direct space have attributed unusual electronic functions for novel devices. These devices are field effect transistors, photodetectors, light emitting diodes (LEDs), quantum cascade lasers, etc.

Recently, new growth techniques have enabled also the synthesis of one-dimensional (1D) nanowire superlattices (NWSLs). NWSLs from groups III–V and group IV elements have been synthesized successfully. InAs/InP superlattices[1] with atomically perfect interfaces and with periods of several nanometers could be realized using techniques, such as molecular beam epitaxy and nanocluster catalyst. Furthermore, compositionally modulated superlattices of GaAs/GaP have been synthesized by laser-assisted catalytic growth technique,[2] again with atomically perfect interfaces and with the component layers ranging from 2 to 21. It is proposed that these NWSLs can offer potential applications in nanoelectronics such as optical nanobar codes, 1D waveguides, and polarized nanoscale LEDs. Longitudinal Si/Si-Ge NWSLs with nanowire diameter ranging from 50 to 300 nm have also been synthesized using laser ablation growth technique.[3] Structural parameters such as nanowire diameter, Ge concentration, and the modulation period in the Si/Si-Ge superlattices can be controlled easily by adjusting the reaction conditions. Technological applications such as LEDs and thermoelectric devices have been suggested. In addition to the longitudinal (axial) nanowire superlattices, coaxial core-shell and core-multishell nanowire heterostructures have attracted interest recently. Crystalline Si/Ge and Ge/Si core-shell structures have been experimentally synthesized by Lauhon *et al.*[4] Most of works involved in 1D superlattices especially concern the experimental synthesis and characterization of coaxial nanowire heterostructures.

Theoretically, only a few works investigated core-shell and longitudinal NWSLs.[5–8] Kagimura *et al.*[6] reported an *ab initio* study of the electronic properties of Si and Ge nanowires and Si/Ge heterostructures with one surface dangling bond state per unit cell. They concluded that surface dangling bond level observed in the band gap of nanowires and nanowire heterostructures can be used as reference level to estimate band lineups in these systems. Using one-band effective mass theory, a criterion has been developed for the occurrence of longitudinal barrier height.[7] It has been argued that radial confinement reduces the actual barrier height in modulated nanowire superlattices. Zypman[8] used the Hubbard model to get the energy spectrum of one-dimensional systems and applied their results to various model systems such as nanowire tunneling diodes and Si/Ge superlattice nanowires to interpret the scanning tunneling spectroscopy measurements. Earlier formation of multiple quantum well structure and resulting confined states on hydrogenated or radially deformed carbon nanotubes have also been reported.[9]

In this paper, we have investigated the mechanical properties and atomic and electronic structures of bare and hydrogenated Si_nGe_n nanowire superlattices using first-principles plane-wave method. NWSLs are constructed from alternating Si and Ge nanowire segments (zones), both have same orientation and similar atomic structure. These segments are joined pseudomorphically and formed a sharp interface. We found that even small diameter hydrogenated Si_nGe_n NWSLs form multiple quantum well structures where conduction and valence band electrons are confined. Our study indicates that the band lineup and resulting electronic structure depend on the length and cross section geometry of the constituent Si_n and Ge_n nanowires.

II. METHOD

We have performed first-principles plane-wave calculations[10,11] within density functional theory (DFT)[12] using ultrasoft pseudopotentials.[11,13] The exchange correlation potential has been approximated by generalized gradient approximation (GGA) using PW91 functional.[14] For partial occupancies, we use the Methfessel-Paxton smearing method.[15] The adopted smearing width is 0.1 eV for the atomic relaxation and 0.02 for the accurate band structure analysis and density of state calculations. All structures have been treated within a supercell geometry using the periodic boundary conditions. The lattice parameters of the tetragonal supercell are a_{sc}, b_{sc}, and c_{sc}. We took $a_{sc}=b_{sc}=27$ Å for NWSL having the largest diameter (~1.8 nm), but $a_{sc}=b_{sc}=22$ Å for one having the smallest diameter (~1.2 nm) considered in this paper. These values allowed minimum distance ranging from ~11 to 14 Å between two atoms in different adjacent cells, so that their coupling is hindered significantly. We took c_{sc} equal to the lattice constant c of the nanowires and NWSLs under consideration. In the self-consistent potential and total energy calculations the Brillouin zone (BZ) is sampled in the **k** space within the Monkhorst-Pack scheme[16] by $(1\times1\times9)$ mesh points for single unit cell and, for example, $(1\times1\times5)$ mesh points for double cells. A plane-wave basis set with kinetic energy of up to 250 eV has been used. All atomic positions and lattice constant $c_{sc}=c$ are optimized by using the conjugate gradient method where total energy and atomic forces are minimized. The criterion of convergence for energy is chosen to be 10^{-5} eV between two ionic steps, and the maximum force allowed on each atom is 0.05 eV/Å.

III. BARE AND HYDROGENATED NANOWIRES AND NANOWIRE SUPERLATTICES

In this study, we considered bare and hydrogen-passivated longitudinal Si_nGe_n nanowire superlattices and also bare and hydrogen-passivated Si and Ge nanowires as constituent structures. Bare Si and Ge nanowires are oriented along the [001] direction of the parent diamond crystal and have normally N atoms in their primitive unit cell with lattice constant c along the nanowire (or z) axis. We took $N=25$ and $N=57$ as two special prototypes. We designate them as SiNW(n) [GeNW(n)] or shortly Si_n (Ge_n) with $n=sN$, s being an integer number. Si_n and Si_N (Ge_n and Ge_N) indicates the same nanowire, except that the unit cell of the former one includes s primitive cell in direct space with $1/s$ times reduced BZ in the momentum space. In our simulations, bare Si_n (Ge_n) nanowires are first cut from the bulk crystal with ideal structural parameters. Subsequently, ideal bare nanowires are relaxed to optimize their structure and lattice constant. Si (Ge) atoms near the core of relaxed nanowire have tetrahedral coordination. To obtain H-passivated Si_n or Ge_n nanowires (designated as H-SiNW(n) or H-GeNW(n), shortly as H-Si_n or H-Ge_n), the dangling bonds at the surface are saturated by H atoms and whole structure is reoptimized. Our study indicates that the atomic and electronic structure of H-Si_n and H-Ge_n may depend on whether hydrogen passivation and subsequent optimization are achieved on ideal or optimized bare Si_n and Ge_n nanowires. The present sequence of structure optimization mimics the actual growth of hydrogen-passivated nanowires.

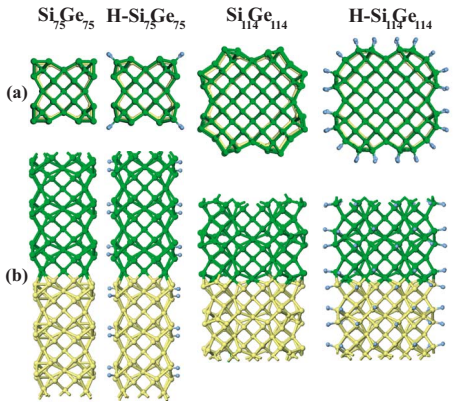

FIG. 1. (Color online) Optimized atomic structure of bare and hydrogenated Si_nGe_n nanowire superlattices for $n=75$ and 114. (a) Top view and (b) side view. Small-gray, large-light, and large-dark balls correspond to the hydrogen, silicon, and germanium atoms, respectively.

A Si_nGe_n has $n=sN$ Si atoms at one side and $n=sN$ Ge atoms at the other side of NWSL unit cell. These atoms have tetrahedral coordination as if they are part of a SiGe heterostructure, and hence at the interface, Si atoms are bonded to Ge atoms pseudomorphically and make atomically flat interface. We note that pseudomorphic growth can sustain for small diameters; but misfit dislocations may be generated at the interface of large diameter (or large N) Si_nGe_n superlattice. Atomic positions and lattice constant are relaxed to obtain optimized structure. H-Si_nGe_n follow the same sequence of construction as H-Si_n or H-Ge_n. Optimized lattice constants of bare Si_nGe_n nanowire superlattice for $n=25$, 50, and 75 are found to have $c=10.9$, 21.8, and 32.7 Å, respectively. Upon hydrogenation, these lattice constants change to $c=11.2$, 22.3, and 33.5 Å, respectively. Lattice constants of bare and hydrogenated Si_nGe_n, $n=57$ and 114, are almost identical and are $c=11.1$ and 22.2 Å, respectively. Figure 1 shows the atomic structure of bare and hydrogen-passivated Si_nGe_n for $n=75$ and 114. These NWSLs are reminiscent of Si_nGe_n (001) planar superlattice, which were fabricated by molecular beam epitaxy by growing first the n Si (001) plane and then n Ge (001) plane and eventually by repeating this Si_nGe_n (001) unit periodically. While the Si_nGe_n (001) superlattice has 2D periodicity in the (001) layers, NWSLs under study here have finite cross section and hence 2D periodicity is absent. Electrons are bound to NWSL in radial (lateral) direction but propagate as 1D Bloch states along the superlattice axis (in longitudinal direction).

Interatomic distance distributions of $Si_{75}Ge_{75}$ and H-$Si_{75}Ge_{75}$ NWSLs are compared with parent Si and Ge nanowires in Fig. 2. In the same figure, we also show the interatomic distance distribution of bare and hydrogenated $Si_{114}Ge_{114}$ NWSL. At the surface, optimized atomic structures of Si_n and Ge_n deviate considerably from the ideal structure of Si_n and Ge_n. For example, one can deduce quad-

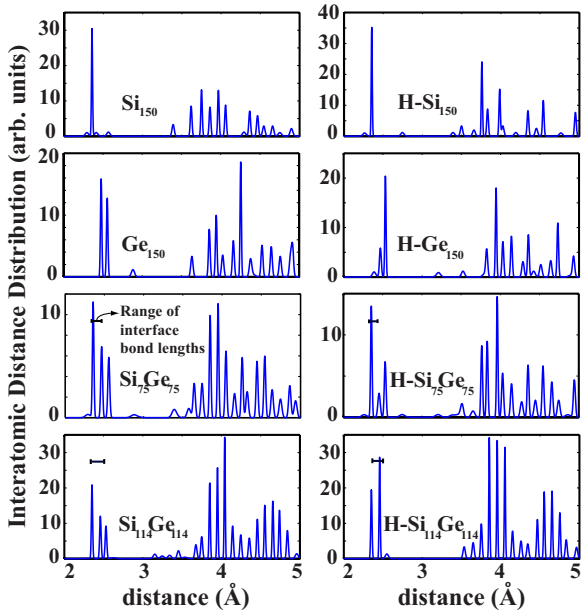

FIG. 2. (Color online) Interatomic distance distribution of optimized bare and hydrogenated Si_{2n}, Ge_{2n}, and Si_nGe_n for $n=75$ up to fourth nearest neighbor. Similar distributions for $Si_{114}Ge_{114}$ and H-$Si_{114}Ge_{114}$ are also shown. The Si-H (Ge-H) bond lengths being in the range of ~1.5 Å are not shown.

rangles of atoms at the surface. Normally, NWSLs consist of hexagonal and pentagonal rings, where one can distinguish bond lengths in different categories. The interatomic distance distribution of Si_nGe_n is reminiscent of the sum of those of Si_{2n} and Ge_{2n} except some changes originated from the interface between Si and Ge segments of supercell. While bulk optimized Si-Si and Ge-Ge bond lengths are $d=2.36$, and 2.50 Å, respectively, the Si-Ge bond at the interface ranges between 2.35 and 2.52 Å for bare $Si_{228}Ge_{228}$ (between 2.37 and 2.49 Å for H-$Si_{228}Ge_{228}$). Nevertheless, the distribution exhibits several peaks corresponding to the deviations from the bulk geometry at the surface. As the cross section or N increases, the effect of the surface decreases and the distribution of interatomic distances becomes more bulklike.

IV. MECHANICAL PROPERTIES

The stability and elastomechanical properties of Si_nGe_n and H-Si_nGe_n NWSLs are crucial for their possible use in nanoelectronics. In the present study, the maximum diameter of nanowire we treated is ~1.8 nm. The diameter of hydrogenated $Si_{25}Ge_{25}$ NWSL is even smaller (~1.4 nm). For such small diameter nanowires or NWSLs, there are ambiguities in determining the area of cross section. Moreover, the surface to volume ratio is rather high and hence makes the cross section nonuniform. In view of these, the calculation of Young's modulus may not be appropriate. Here, we rather considered the force (spring) constants of nanowires and NWSLs under a strain in the harmonic region. To this end, we calculated the second derivative of the total energy (per unit cell) with respect to the lattice constant c (i.e., $\kappa = d^2E_T/dc^2$) or to the strain, $\epsilon=\Delta c/c$ (i.e., $\kappa' = d^2E_T/d\epsilon^2$).

TABLE I. Equilibrium values of lattice parameter c are given in units of Å. Force constant κ (as defined in the text), in units of eV/Å, is calculated by using both VASP result and Hook's law. Percentage difference in between force constant values calculated from VASP result and Hook's law is given within parenthesis in order to check whether classical Hook's law is still valid in nanoscale. Also force constant κ' (as defined in the text) is presented in units of eV.

Structure	c_0	κ	Hook's law		κ'
Si_{25}	5.32	5.68			161
Ge_{25}	5.57	3.28			102
$Si_{25}Ge_{25}$	10.90	2.18	2.08	(5)	259
$Si_{50}Ge_{50}$	21.75	0.92	1.04	(12)	437
$Si_{75}Ge_{75}$	32.70	0.62	0.69	(10)	663
Si_{57}	5.43	11.22			327
Ge_{57}	5.65	7.49			239
$Si_{57}Ge_{57}$	11.07	4.24	4.49	(6)	522
$Si_{114}Ge_{114}$	22.15	2.10	2.25	(7)	1035
H-Si_{25}	5.45	8.56			254
H-Ge_{25}	5.73	5.98			196
H-$Si_{25}Ge_{25}$	11.17	3.48	3.52	(1)	436
H-$Si_{50}Ge_{50}$	22.30	1.70	1.76	(3)	845
H-$Si_{75}Ge_{75}$	33.50	1.14	1.17	(3)	1279
H-Si_{57}	5.39	13.57			394
H-Ge_{57}	5.68	11.09			358
H-$Si_{57}Ge_{57}$	11.05	6.13	6.10	(1)	755
H-$Si_{114}Ge_{114}$	22.08	3.33	3.05	(8)	1626

The values calculated for nanowires and NWSLs treated in our paper are given in Table I.

Like bulk crystals, Si_n nanowires are stiffer than Ge_n nanowires. This implies that the lattice mismatch between Si and Ge nanowires in NWSL is accommodated mainly by the Ge zone. For both nanowires and NWSL, κ increases with increasing cross section. For example, κ of Si_{25} is almost the half of κ of Si_{57}. Note that $\kappa(Si_{50}) \simeq \kappa(Si_{25})/2$. As for κ of $Si_{25}Ge_{25}$ NWSL calculated from first principles is 2.18 eV/Å. This value can be estimated in terms of two springs connected in series, namely, $\kappa^{-1}(Si_{25}Ge_{25}) \simeq \kappa^{-1}(Si_{25}) + \kappa^{-1}(Ge_{25})$ to be $\kappa(Si_{25}Ge_{25}) \simeq 2.08$ eV/Å. We, therefore, conclude that as long as the geometry and size of the cross section remained to be similar, classical Hook's law continues to be approximately valid even for nanostructures. Upon hydrogenation, both nanowires as well as NWSLs studied here become stiffer. The spring constant of $Si_{57}Ge_{57}$ is twice that of $Si_{114}Ge_{114}$ because the latter NWSL has twice the length of the former. We also calculated[18] the ratio of the strain of the Ge zone to that of Si zone of $Si_{75}Ge_{75}$ under tensile stress, i.e., $\epsilon(Ge)/\epsilon(Si)$ to be ~2.5. This ratio is reduced to ~1.25 for $Si_{114}Ge_{114}$. In compliance with the κ values in Table I, this result indicates that in a Si_nGe_n, NWSL Ge zone elongates more than Si zone. Using empirical potential, Menon *et al.*[17] were able to calculate the Young's modulus and bending stiffness of tetrahedral and cagelike Si nanowire of ~4 nm diameter and found values comparable with bulk values.

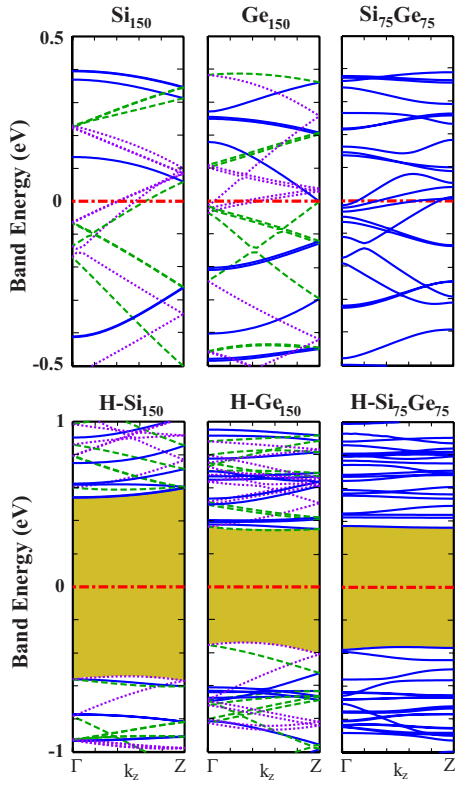

FIG. 3. (Color online) Energy band structures of optimized bare and hydrogenated Si_{2n}, Ge_{2n} nanowires, and Si_nGe_n nanowire superlattices for $n=75$. Zero of energy is taken at the Fermi level. Band gaps are shown by shaded zones. Dashed and dotted lines (minibands) are obtained by folding of Si_{50} (also H-Si_{50}) and Ge_{50} (also H-Ge_{50}) bands.

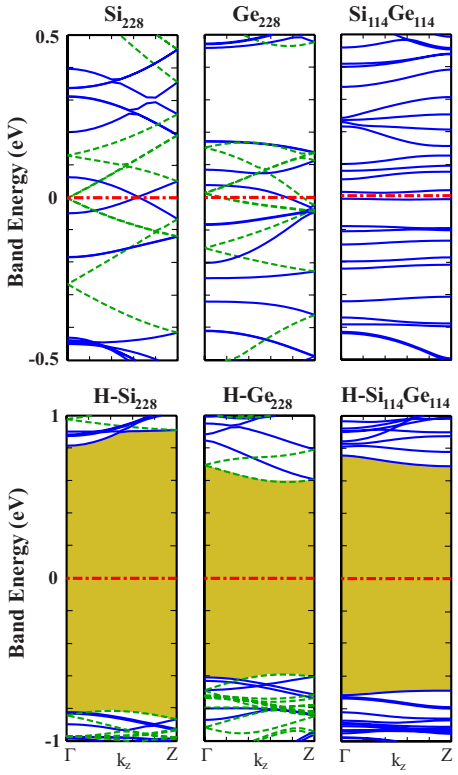

FIG. 4. (Color online) Energy band structures of optimized bare and hydrogenated Si_{2n}, Ge_{2n} nanowires, and Si_nGe_n nanowire superlattices for $n=114$. Zero of energy is taken at the Fermi level. Dashed and dotted lines are obtained by folding of Si_{57} (also H-Si_{57}) and Ge_{57} (also H-Ge_{57}) bands.

V. ELECTRONIC PROPERTIES

The band structures of optimized bare and hydrogenated Si_nGe_n are given in Figs. 3 and 4 for $n=75$ and 114, respectively. In the same figures, the band structures of bare and hydrogenated Si_{2n} and Ge_{2n} constituent nanowires are presented for the sake of comparison. Si_N ($N=25$ and 57) and hence any Si_{2n} ($n=sN$) nanowires are metallic due to the surface dangling bonds. Similarly, Ge_N ($N=25$ and 57) and hence any Ge_{2n} are metallic. Upon passivation of dangling bonds, these metallic nanowires become semiconductor. For example, H-Si_{150} and H-Ge_{150} nanowires have indirect band gaps, $E_g=1.1$ and 0.7 eV, respectively. Normally, the band gap of a H-Si_n is inversely proportional to its diameter, if the corresponding ideal nanowire cut from the bulk crystal was directly passivated with H before the structural optimization. Also, the band gap is affected by the cross section geometry for small N. For large N, the variation of E_g with N is more uniform.

Like Si_{150} and Ge_{150}, $Si_{75}Ge_{75}$ is metallic. The ideal equilibrium ballistic conductances of Si_{150}, Ge_{150} nanowires, and $Si_{75}Ge_{75}$ NWSL are revealed to be $6e^2/h$, $10e^2/h$, and $8e^2/h$, respectively. Since H-Si_{150} and H-Ge_{150} are semiconductors, H-$Si_{75}Ge_{75}$ NWSL is also semiconductor: Its band gap is 0.7 eV and close to the band gap of H-Ge_{150}. H-$Si_{114}Ge_{114}$ has a direct band gap of 1.4 eV. Again, it is smaller than the band gap of H-Si_{228} but closer to that of H-Ge_{228}.

In Fig. 5, we examine how the electronic energy bands of nanowire superlattices evolve with the lattice constant c or s. In the case of $N=25$, bare Si_nGe_n nanowire superlattices are metallic for all n ($n=25$ and 50 or $s=1$, 2, and 3). As s increases, additional minibands occur and they become flatter. As for H-Si_nGe_n, they are all semiconductor for $n=25$, 50, and 75. As n increases, all bands including lowest conduction and highest valence band become flatter with the formation of minibands. In this respect, the band gap becomes more uniform as s increases. Similar behaviors are

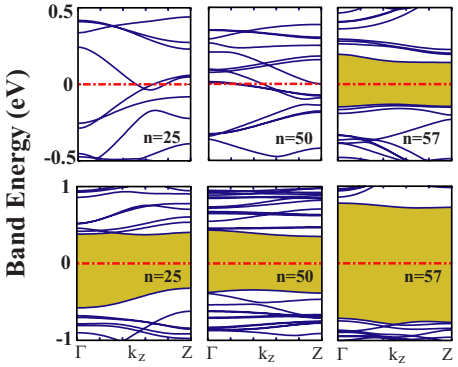

FIG. 5. (Color online) Energy band structure of bare and hydrogenated Si_nGe_n nanowire superlattices for $n=25$, 50, and 57.

displayed also for H-Si_nGe_n with $n=57$ and 114 (see Fig. 4). Unexpectedly, bare Si_nGe_n are semiconducting for $n=57$ and 114. The band gap decreases from 0.27 to 0.02 eV as s increases from 1 to 2. Isosurface charge densities of these states near the band gap edges found that they are confined in one of the zones. It is concluded that opening of the band gap originates from the mismatch of surface dangling bond states in Si and Ge zones.

It should be noted that the band gap is underestimated by the GGA calculations used in the present study. *GW* correction performed recently[20] for H-Si_n in different orientations is in the range of 0.5–0.6 eV for large diameters. In view of the fact that Ge bulk is predicted as metal by GGA calculation, *GW* correction for H-Ge_n nanowires is expected to be in the same range as that for H-Si_n. Under these circumstances, a scissor operation (namely, increasing the band gap of corresponding Si_nGe_n by the same amount of 0.5–0.6 eV) may yield the actual band gap. In summary, the band gaps of H-Si_nGe_n predicted by GGA calculation are underestimated, and actual bands are expected to be 0.5–0.6 eV larger.

VI. CONFINED STATES

The results discussed in the previous section reveal that Si_n and Ge_n nanowires making a Si/Ge heterojunction in the supercell have band gaps of different widths. Upon a pseudomorphic junction, the bands and hence band gaps corresponding to Si and Ge zones are aligned. Combination of two features, namely, Si and Ge zones having different band gaps and band lineup, results in band discontinuities and hence band offsets. The conduction and valence band edges of different zones (Si zone or Ge zone) in the nanowire superlattice will have different energies. Under these circumstances, the diagram of the conduction band edge along the axis of NWSL will display a multiple quantum well structure with the periodicity of c_{sc} like a Kronig-Penny model. Electrons in the well region of a zone should decay in the adjacent zones having higher conduction band edge, since their energy will fall into the band gap of this barrier zone. As a result, the states of these confined (or localized) electrons are propagating in the well, but decaying in the barrier. Usually, confined electrons have low group velocity. They may become more localized if the barrier is high and the width of barrier is large. If the confinement (or localization) is complete, the associated band $E_n(k_z)$ becomes flat.[19] Similar arguments are valid for the hole states if the energies of valence band edges of both zones are different.

In the past, the reference energies in determining band offsets of 2D superlattices have been actively studied both experimentally and theoretically. Energy diagrams of conduction and valence band edges are then used as effective potential forming a multiple quantum well structure.[21] The states of conduction band electrons and holes of valence band were treated using effective mass theory (EMT). These states are free electronlike 2D bands in the planes and Bloch states forming minibands perpendicular to the planes. The conditions are, however, different in NWSLs. First of all, EMT may not be applicable directly in the present case, in particular, for NWSLs with small diameter. Second, the reference energy level determined for planar superlattices may not be appropriate. Recently, Kagimura *et al.*[6] proposed surface dangling bond states as reference level for Si/Ge core-shell superlattices. Under estimation of band gaps by DFT, GGA calculation may hinder the accurate determination of band lineups. Voon and Willatzen[7] drew attention to the lateral confinement of states in NWSLs. Using one-band EMT and by solving the Ben Daniel–Duke[22] equation, they found that the effective barrier is lowered due to the coupling between radial and longitudinal confinements. In particular, they predicted that the effective barrier and hence confinement disappear below a critical radius of ~5 nm. In the present study, the maximum radius of NWSL was ~0.9 Å which is much lower than the critical radius set for GaAs/AlGaAs NWSLs.[7]

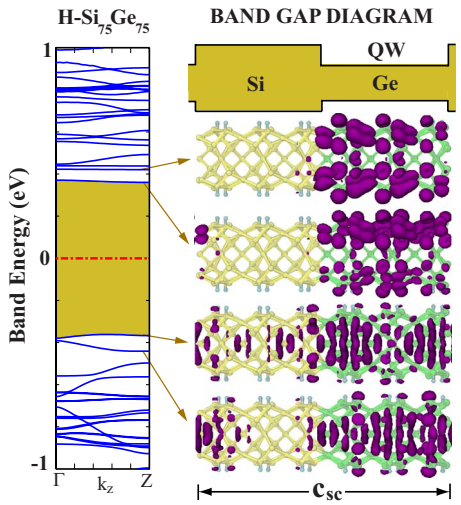

FIG. 6. (Color online) Schematic description of energy band diagram in the unit cell (on the right and upper side), band structure in the momentum space (on the left side), and isosurface charge density of states of H-$Si_{75}Ge_{75}$ NWSL at the band edges.

In the present study, we examined whether some of states can be longitudinally confined by performing an extensive analysis of charge densities of superlattice bands calculated by first-principles methods. The formation of periodic quantum well structure is schematically described in Fig. 6. We expect that the values of band gaps in the H-Si and H-Ge zones in a unit cell of the H-$Si_{75}Ge_{75}$ cannot deviate significantly from the values calculated for periodic H-Si_{25} and H-Ge_{25} nanowires (namely, 1.1 and 0.7 eV, respectively). When the two zones are connected by an atomically flat interface, H-Ge zone can form a well between adjacent H-Si zones, since the band gap of the former zone is smaller and the energy of conduction band edge is lower relative to that of the latter zone. Upon normal band lineup, H-Ge_{75} zone acts as a quantum well for both lowest conduction and highest valence band electrons. Band structure of H-$Si_{75}Ge_{75}$ with two lowest conduction and two highest valence minibands and their isosurface charge distribution in the superlattice unit cell are shown in Fig. 6. The distribution of electronic charge density is confirming the above normal band lineup. Both conduction band states are confined in the H-Ge_{75} zone, but they have very small weight in the H-Si_{75}

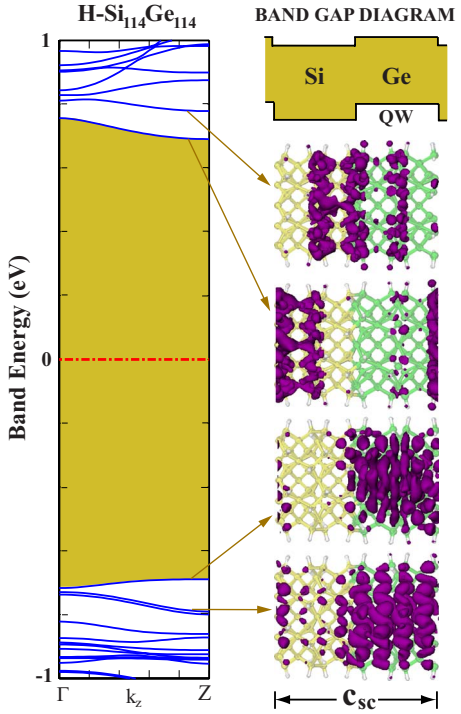

FIG. 7. (Color online) Schematic description of energy band diagram in the unit cell (on the right and upper side), band structure in the momentum space (on the left side), and isosurface charge density of states of H-$Si_{114}Ge_{114}$ NWSL at the band edges.

zone. Similarly, states corresponding to two highest valence bands are also confined in the H-Ge_{75} zone. It should be noted that owing to the charge transfer between adjacent zones the form of the energy band diagram may change from the simple form given in Fig. 6.

In Fig. 7, we present similar analysis for H-$Si_{114}Ge_{114}$ NWSL. As compared to H-$Si_{75}Ge_{75}$, here H-Si and H-Ge zones are ~5 Å shorter. However, there are more minibands owing to larger number of Si and Ge atoms. The ways the highest valence band and the lowest conduction band states are confined in different zones suggest a staggered band lineup. Highest valence band states are confined in the H-Ge zone; but lowest conduction band states are confined in H-Si zone. States of sixth and seventh valence bands (from the top) are propagating throughout the NWSL.

We believe that present *ab initio* results revealing confined states for NWSLs with a radius as small as ~0.6 nm are not contradicting the conclusions obtained from one-band EMT model. We think that EMT as applied in Ref. 7 has to be revised for small diameter NWSL.[23] We also note that H-Si_nGe_n nanowire superlattice has 1D rodlike structure. There are several minibands in the 1D BZ. The number of minibands in a given energy interval increases with either increasing N (i.e., increasing diameter) or increasing s. A nanowire superlattice with a long unit cell having several Si or Ge atoms will have several (quasi continuous) minibands. States of H-Si_n or H-Ge_n zone of the same energy are more likely to match each other to construct a state that propagate throughout the NWSL. Otherwise, a superlattice of small radius with short unit cell has small number of bands. Then, the states in different zones are less likely to match. A state, which cannot find a matching partner, is confined to its zone. As a matter of fact, we were able to deduce confined states even in the barrier zone (H-Si) with energies higher than the conduction band edge.

VII. CONCLUSION

Atomic structure of H-Si_n and H-Ge_n nanowires is tetrahedrally coordinated near the center, but at the surface deviates significantly from corresponding bulk crystal. Calculated force constants indicate that Si_n is stiffer than Ge_n. Generally, nanowires become stiffer after passivation with hydrogen. These two nanowires are 1D semiconductors with their band gap depending on their diameter and also on the geometry of their relaxed cross section. If finite segments of these nanowires are joined pseudomorphically and the resulting heterostructure are repeated periodically along the axis of the wires, one obtains a H-Si_nGe_n superlattice structure. In these longitudinal NWSLs, electrons are normally bound to the wire in radial direction, but propagate along their axis. A specific state which propagates in one zone (say H-Si) can decay in the adjacent zone (say H-Ge), when a matching state in the same energy is absent. Such a state is called confined state. Our charge density analyses indicate that Si/Ge NWSL with radius as small as 0.6 nm can have confined states at the band edges and also within the conduction and valence band. Confined states offer interesting device applications. NWSL has an important advantage that the device part and leads can be produced from similar nanowires. Theoretically, NWSLs have several interesting issues to be clarified. In particular, theories derived from planar superlattices to predict band lineups and model calculations using EMT have to be revised for small diameter NWSLs.

*ciraci@fen.bilkent.edu.tr

[1] M. T. Bjork, B. H. Ohlsson, T. Sass, A. I. Persson, C. Thelander, M. H. Magnusson, K. Deppert, L. R. Wallenberg, and L. Samuelson, Nano Lett. **2**, 87 (2002).
[2] M. S. Gudiksen, L. J. Lauhon, J. Wang, D. C. Smith, and C. M. Lieber, Nature (London) **415**, 617 (2002).
[3] Y. Wu, R. Fan, and P. Yang, Nano Lett. **2**, 83 (2002).
[4] L. J. Lauhon, M. S. Gudiksen, D. Wang, and C. M. Lieber, Nature (London) **420**, 57 (2002).
[5] R. N. Musin and X.-Q. Wang, Phys. Rev. B **71**, 155318 (2005).
[6] R. Kagimura, R. W. Nunes, and H. Chacham, Phys. Rev. Lett. **98**, 026801 (2007).
[7] L. C. Lew, Yan Voon, and M. Willatzen, J. Appl. Phys. **93**, 9997 (2003).
[8] F. R. Zypman, Phys. Rev. B **71**, 165313 (2005).
[9] O. Gulseren, T. Yildirim, and S. Ciraci, Phys. Rev. B **68**, 115419

(2003); C. Kilic, S. Ciraci, O. Gulseren, and T. Yildirim, *ibid.* **62**, R16345 (2000).

[10] M. C. Payne, M. P. Teter, D. C. Allen, T. A. Arias, and J. D. Joannopoulos, Rev. Mod. Phys. **64**, 1045 (1992).

[11] Numerical computations have been carried out by using VASP software: G. Kresse and J. Hafner, Phys. Rev. B **47**, R558 (1993); G. Kresse and J. Furthmuller, *ibid.* **54**, 11169 (1996).

[12] W. Kohn and L. J. Sham, Phys. Rev. **140**, A1133 (1965); P. Hohenberg and W. Kohn, Phys. Rev. **136**, B864 (1964).

[13] D. Vanderbilt, Phys. Rev. B **41**, R7892 (1990).

[14] J. P. Perdew, J. A. Chevary, S. H. Vosko, K. A. Jackson, M. R. Pederson, D. J. Singh, and C. Fiolhais, Phys. Rev. B **46**, 6671 (1992).

[15] M. Methfessel and A. T. Paxton, Phys. Rev. B **40**, 3616 (1989).

[16] H. J. Monkhorst and J. D. Pack, Phys. Rev. B **13**, 5188 (1976).

[17] M. Menon, D. Srivastava, I. Ponomareva, and L. A. Chernozatonskii, Phys. Rev. B **70**, 125313 (2004).

[18] These calculations have been performed by minimizing the total energy under a preset uniaxial strain in the elastic range. The strains on Ge and Si zones calculated are determined after full relaxation.

[19] Accordingly, such a state has $\int_{well}\Psi_c^*\Psi_c d\vec{r} \gg \int_{barrier}\Psi_c^*\Psi_c d\vec{r}$. If the confinement is complete, electrons in adjacent levels do not interact. This is known as the Mott localization.

[20] X. Zhao, C. M. Wei, L. Yang, and M. Y. Chou, Phys. Rev. Lett. **92**, 236805 (2004).

[21] L. Esaki and L. L. Chang, Phys. Rev. Lett. **33**, 495 (1974).

[22] G. Bastard, *Wave Mechanics Applied to Semiconductor Heterostructures* (Les Editions de Physique, Les Ulis, 1988).

[23] We also note that the material parameters of GaAs/AlGaAs relevant for EMT by themselves are different from Si_nGe_n nanowire superlattices studied here.